

Extraordinarily High Activity in the Hydrodesulfurization of 4,6-Dimethyldibenzothiophene over Pd Supported on Mesoporous Zeolite Y

Wenqian Fu,[†] Lei Zhang,[†] Tiandi Tang,^{*,†} Qingping Ke,[†] Shun Wang,[†] Jianbo Hu,[†] Guoyong Fang,[†] Jixue Li,[#] and Feng-Shou Xiao^{*,†}

[†]College of Chemistry and Materials Engineering, Wenzhou University, Wenzhou 325027, P. R. China

[‡]Department of Chemistry, Zhejiang University, Hangzhou 310028, P. R. China

[#]Electron Microscopy Centre, Zhejiang University, Hangzhou 310027, P. R. China

S Supporting Information

ABSTRACT: Design and preparation of highly active hydrodesulfurization (HDS) catalysts is very important for the removal of air pollution. Herein, we report an extraordinarily active HDS catalyst, which is synthesized by loading of Pd on mesoporous zeolite Y (Pd/HY-M). The mesoporous zeolite Y is successfully synthesized using a water glass containing *N,N*-dimethyl-*N*-octadecyl-*N*-(3-triethoxysilylpropyl) ammonium $[(C_2H_5O)_3SiC_3H_6N(CH_3)_2C_{18}H_{37}]^+$ cation as a mesoscale template. Compared with mesoporous Beta and ZSM-5 supported Pd catalysts (80.0% and 73.4% for Pd/HBeta-M and Pd/HZSM-5-M, respectively) as well as commercial catalyst of γ -Al₂O₃ supported Pd catalyst (31.4%), Pd/HY-M catalyst exhibited very high activity in HDS of 4,6-dimethyldibenzothiophene (4,6-DM-DBT, 97.3%). The higher activity of Pd/HY-M than that of Pd/HBeta-M and Pd/HZSM-5-M is assigned to the larger micropore size of zeolite Y compared to that of Beta and ZSM-5. Theoretical simulation and adsorption experimental data show that 4,6-DM-DBT has difficulty entering the micropores of ZSM-5 and Beta zeolites, but the micropores of Y zeolite are accessible.

The reduction of the sulfur content in diesel fuel has received much attention in recent years owing to stringent environmental legislations in many countries for a sulfur level less than 10 ppm.¹ To reach this low level, complete removal of highly refractory molecules such as 4,6-dimethyldibenzothiophene (4,6-DM-DBT) is inevitable.¹ However, conventional supported metal sulfides have difficulty fully removing 4,6-DM-DBT, due to steric hindrance by the methyl groups adjacent to the sulfur atom,² and the solution for this problem is to increase hydrogenating ability and support acidity of the catalysts.³ Recently, Sun and Prins⁴ reported high activity in 4,6-DM-DBT hydrodesulfurization (HDS) over noble metals supported on mesoporous ZSM-5 zeolite. The replacement of metal sulfides by noble metals strongly enhanced the hydrogenating ability, and the use of strongly acidic zeolite support was favorable for lowering the sulfur sensitivity of the metal.⁵ Moreover, strong acidity is also helpful for spillover of hydrogen atoms from the metal particles to the aromatic sulfur-containing molecules, which could create a second

hydrogenation pathway.⁶ Nevertheless, in these mesoporous ZSM-5 and Beta zeolite supported noble metal catalysts, HDS occurs in the mesopores, because bulky 4,6-DM-DBT molecules cannot diffuse into the pores of ZSM-5 (pore size of 0.55 nm) and Beta (pore size of 0.65–0.68 nm) zeolites.^{4,7}

From a theoretical simulation, we estimated the molecular size of 4,6-DM-DBT to be 0.78 × 1.13 nm (Table S1), which is comparable with the microporosity of zeolite Y (window of 0.74 nm and supercage of 1.3 nm). Therefore, 4,6-DM-DBT can enter the micropores of zeolite Y under HDS conditions. This is supported by adsorption of 4,6-DM-DBT on zeolite Y supported Pd catalyst (74.8 mg/g Cat., Table S2). Herein, we report the synthesis of mesoporous zeolite Y by templating with a mesoscale silane surfactant and the HDS of 4,6-DM-DBT over a Pd catalyst supported on the mesoporous zeolite Y. Compared with mesoporous ZSM-5 and Beta or conventional γ -Al₂O₃, mesoporous zeolite Y supported Pd catalyst exhibits extraordinarily high activity for HDS.

Notably, despite much encouraging progress for the successful synthesis of mesoporous ZSM-5 and Beta zeolites by using mesoscale organic templates,⁸ it is still difficult to obtain mesoporous zeolite Y by the same route, due to the difficulty of dispersing the organic templates into the viscous gel used in the synthesis of zeolite Y.⁸ In this work, we systemically investigated the dispersion of mesoscale templates in the starting gel, and found that a silane of *N,N*-dimethyl-*N*-octadecyl-*N*-(3-triethoxysilylpropyl) ammonium bromide $[(C_2H_5O)_3SiC_3H_6N(CH_3)_2C_{18}H_{37}]Br$, TPOAB) could be highly dispersed in water glass, a raw material for synthesizing zeolite Y. Replacement of conventional water glass by TPOAB-dispersed water glass in the synthesis resulted in the formation of mesoporous zeolite Y, which was designated as NaY-M sample.

Figure 1 shows the X-ray diffraction (XRD) pattern, nitrogen isotherm, scanning electron microscopy (SEM) image, and transmission electron microscopy (TEM) image of the NaY-M sample. The XRD pattern gives well-resolved peaks in the range 4–40° with zeolite Y structure (Figure 1a). The nitrogen isotherm of calcined NaY-M exhibits a step at a relative pressure of 0.4–0.96, which is typically assigned to the presence of mesostructure (Figure 1b). Correspondingly, the pore-size distribution for

Received: August 3, 2011

Published: September 13, 2011

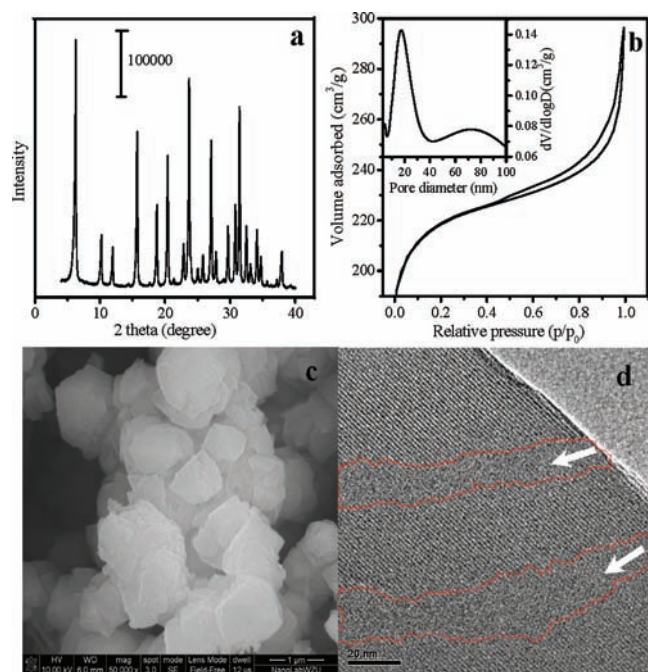


Figure 1. (a) XRD pattern, (b) N_2 isotherm, (c) SEM image, and (d) TEM image of NaY-M sample (the mesoporosity in the crystal was marked by red lines and white arrows).

Table 1. Textural parameters of supports and CO-chemisorption data of the corresponding catalysts

samples	S_{BET} (m^2/g) ^a	S_{ext} (m^2/g) ^b	V_{meso} (cm^3/g) ^c	CO-ad. Pd catalysts ^d	
				D (%)	d (nm)
NaY-M	859	137	0.20	36	3.1
HY-M ^e	841	142	0.21	50	2.3
HY ^e	904	72	0.08	37	3.0
HBeta-M ^e	551	144	0.24	36	3.1
HZSM-5-M ^e	453	170	0.19	37	3.0
$\gamma\text{-Al}_2\text{O}_3$	320	320	0.47	56	1.9

^a BET surface area. ^b External surface area. ^c Mesoporous pore volume.

^d Dispersion and particle size of Pd nanoparticles estimated from CO-chemisorption data (D and d stand for dispersion and particle size, respectively). ^e The Si/Al ratios of HY-M, HY, HZSM-5-M, and HBeta-M at 2.6, 2.5, 19.6 and 18.4, respectively.

calcined NaY-M shows mesopores in the range 8–30 nm, centered at 18 nm (inset, Figure 1b). The SEM image of the calcined NaY-M (Figure 1c) exhibits the particles ranged at 0.7–1.5 μm with similar morphology. The TEM image at high magnification gives direct evidence for the presence of mesopores (Figure 1d, 10–25 nm) in the sample.

After ion-exchange of NaY-M with a NH_4NO_3 aqueous solution and calcination at 550 $^\circ\text{C}$, the H-form of zeolite Y was obtained (HY-M). Then, Pd nanoparticles were loaded, forming a mesoporous zeolite Y supported Pd catalyst (Pd/HY-M). In comparison, we also prepared mesoporous ZSM-5 (HZSM-5-M) and Beta (HBeta-M) supported Pd catalysts. Table 1 presents textural parameters and CO-chemisorption data of the various

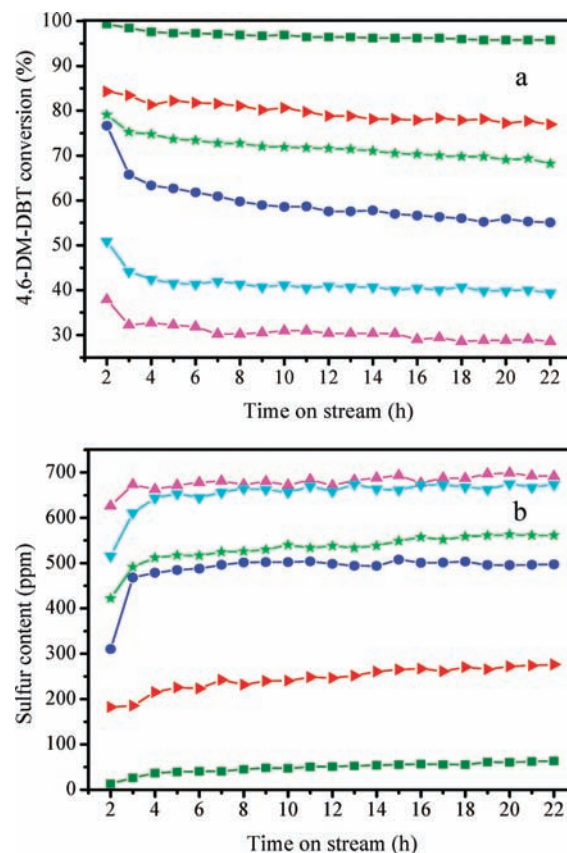


Figure 2. Dependence of the 4, 6-DM-DBT conversion (a) and the remaining sulfur content (b) in 4,6-DM-DBT-hydrogenation system on reaction time over (green ■) Pd/HY-M, (red ►) Pd/HBeta-M, (green ★) Pd/HZSM-5-M, (blue ●) Pd/HY, (turquoise ▼) Pd/NaY-M, and (pink ▲) Pd/ $\gamma\text{-Al}_2\text{O}_3$ catalysts.

samples. The mesoporous zeolites of the HY-M, HZSM-5-M, and HBeta-M have similarly large external surface areas (142–170 m^2/g) and mesopore volumes (0.19–0.24 cm^3/g), which are still smaller than those (320 m^2/g and 0.47 cm^3/g) of $\gamma\text{-Al}_2\text{O}_3$. The Pd nanoparticles on the zeolite supports, estimated by CO-chemisorption, was 2.3–3.1 nm, which is slightly larger than those (1.9 nm) on the $\gamma\text{-Al}_2\text{O}_3$ support. The Pd particles are located in both disordered mesopores (Figures S1 and S5) and ordered micropores (Figures S2–S4), which are attributed to the fact that NaY-M sample contains both hierarchical mesopores (8–30 nm) and ordered micropores (0.74 nm). Curves of temperature-programmed desorption of ammonia show that the H-form of zeolite supports have strong acidic sites, while the acidity of NaY-M and $\gamma\text{-Al}_2\text{O}_3$ is relatively weak (Figure S6).

Figure 2 shows the dependences of 4,6-DM-DBT conversion and the remaining sulfur content on the reaction time over the various catalysts. Conventional Pd/ $\gamma\text{-Al}_2\text{O}_3$ shows relatively low conversion (34.1% at 6 h). Weakly acidic Pd/NaY-M catalyst also gives low conversion (41.3% at 6 h).

When acidic HZSM-5-M is used as support, Pd/HZSM-5-M exhibits higher activity, reaching 73.4% at 6 h. The higher activity is assigned to the contribution of strong acidity and mesoporosity in the support, in good agreement with those previously reported by Sun et al.⁴ Very interestingly, strongly acidic Pd/HY-M catalyst shows the highest activity, giving a conversion of 97.3% at 6 h. As a result, remaining sulfur

content in the liquid phase is only 40 ppm over Pd/HY-M catalyst. Considering the similarity of Pd/HY-M, Pd/HZSM-5-M and Pd/HBeta-M for mesoporosity, external surface area, and strong acidity as well as Pd loading and nanoparticle sizes, the much higher catalytic activity in HDS of 4,6-DM-DBT over Pd/HY-M than over Pd/HZSM-5-M and Pd/HBeta-M should be directly assigned to the difference in microporosity in the samples. HY-M has relatively large micropores, which could be accessible for bulky 4,6-DM-DBT. On the contrary, 4,6-DM-DBT molecules have difficulty entering the micropores of HZSM-5-M and HBeta-M.^{36,4} This suggestion is supported by 4,6-DM-DBT adsorption experiments, which show the adsorption capacity of Pd/HY (74.8 mg/g) is much higher than that of Pd/HZSM-5 (11.2 mg/g) and Pd/HBeta (26.8 mg/g, Table S2), confirming that the micropores of HY are more favorable for access of 4,6-DM-DBT than those of ZSM-5 and Beta. On the other hand, mesoporosity in the samples is also a critical factor for enhancing catalytic activity. For example, Pd/HY shows a conversion of 61.8% at 6 h. However, after introduction of mesoporosity in HY, Pd/HY-M gives a very high conversion of 97.3% at 6 h. These results could be related to the presence of mesoporosity in the samples, which is favorable for mass transfer and access for bulky 4,6-DM-DBT. Clearly, the support of HY-M perfectly combines the advantages of mesoporosity with large micropore size, leading to the highest activity in HDS during all supported Pd catalysts.

It has been reported that 4,6-DM-DBT over Pd catalysts can be hydrogenated to sulfur-containing intermediates such as 4,6-dimethylhexahydrodibenzothiophene (DM-HH-DBT),⁴ which could be desulfurized to hydrocarbons by the direct desulfurization (DDS) and hydrogenation pathways (HYD),⁴ as proposed in Scheme S1. Table S3 presents product selectivity in the HDS of 4,6-DM-DBT at a reaction time of 6 h. The results suggest that the intermediate of DM-HH-DBT from HDS of the 4,6-DM-DBT over strongly acidic catalysts (e.g., Pd/HY-M) is more favorable for hydrogenating the DM-HH-DBT to DM-PH-DBT forming DM-BCH by DDS route than that over relatively weak acidic catalysts (e.g., Pd/ γ -Al₂O₃).

In summary, mesoporous zeolite Y is successfully synthesized using TPOAB as a mesoscale organic template. After loading Pd on the H-form of mesoporous zeolite Y, the resulting catalyst shows a very high activity in the HDS of 4,6-DM-DBT compared with HZSM-5-M and HBeta-M or γ -Al₂O₃ supported Pd catalysts. This phenomenon is assigned to a combination of the advantages for the mesoporosity and large micropores in HY-M. The mesoporosity is favorable for mass transfer, and the micropores are accessible for bulky 4,6-DM-DBT. The mesoporous zeolite Y supported noble metal catalysts would be potentially important for a removal of sulfur content in diesel fuel by HDS route in the future.

■ ASSOCIATED CONTENT

S Supporting Information. Experimental details, catalyst test, characterization, theoretical simulation, adsorption experiments and the product selectivity of the HDS. This material is available free of charge via the Internet at <http://pubs.acs.org>.

■ AUTHOR INFORMATION

Corresponding Author

tangtd2006@yahoo.com.cn; fsxiao@zju.edu.cn

■ ACKNOWLEDGMENT

This work was supported by the National Natural Science Foundation of China (21076163), the Natural Science Foundation of Zhejiang Province of China (Y4090084 and Y4100580).

■ REFERENCES

- (1) (a) Yang, R. T.; Hernández-Maldonado, A. J.; Yang, F. H. *Science* **2003**, *301*, 79–81. (b) Song, C. *Catal. Today* **2003**, *86*, 211–263. (c) Torres-Nieto, J.; Brennessel, W. W.; Jones, W. D.; García, J. J. *J. Am. Chem. Soc.* **2009**, *131*, 4120–4126. (d) Buccella, D.; Janak, K. E.; Parkin, G. J. *Am. Chem. Soc.* **2008**, *130*, 16187–16189. (e) Sattler, A.; Parkin, G. *Nature* **2010**, *463*, 523–526. (f) Sattler, A.; Parkin, G. *J. Am. Chem. Soc.* **2011**, *133*, 3748–3751.
- (2) (a) Houalla, M.; Nag, N. K.; Sapre, A. V.; Broderick, D. H.; Gates, B. C. *AIChE J.* **1978**, *24*, 1015–1021. (b) Girgis, M. J.; Gates, B. C. *Ind. Eng. Chem. Res.* **1991**, *30*, 2021–2058. (c) Gates, B. C.; Topsøe, H. *Polyhedron* **1997**, *16*, 3213–3217. (d) Kabe, T.; Ishihara, A.; Zhang, Q. *Appl. Catal., A* **1993**, *97*, L1–L9. (e) Meille, V.; Schulz, E.; Lemaire, M.; Vrinat, M. *J. Catal.* **1997**, *170*, 29–36. (f) Bataille, F.; Lemberton, J. L.; Michaud, P.; Pérot, G.; Vrinat, M.; Lemaire, M.; Schulz, E.; Breyse, M.; Kasztelan, S. *J. Catal.* **2000**, *191*, 409–422. (g) Bej, S. K.; Maity, S. K.; Turaga, U. T. *Energy Fuels* **2004**, *18*, 1227–1237. (h) Shu, Y.; Lee, Y. K.; Oyama, S. T. *J. Catal.* **2005**, *236*, 112–121. (i) Li, X.; Wang, A.; Egorova, M.; Prins, R. J. *Catal.* **2007**, *250*, 283–293. (j) Lauritsen, J. V.; Kibsgaard, J.; Helveg, S.; Topsøe, H.; Clausen, B. S.; Lægsgaard, E.; Besenbacher, F. *Nat. Nanotechnol.* **2007**, *2*, 53–58. (k) Topsøe, H. *Appl. Catal., A* **2007**, *322*, 3–8. (l) Wang, H.; Prins, R. J. *Catal.* **2009**, *264*, 31–43.
- (3) (a) Corma, A.; Martínez, A.; Martínez-Soria, V. J. *Catal.* **1997**, *169*, 480–489. (b) Reinhoudt, H. R.; Troost, R.; van Schalkwijk, S.; van Langeveld, A. D.; Sie, S. T.; Schulz, H.; Chadwick, D.; Cambra, J.; de Beer, V. H. J.; van Veen, J. A. R.; Fierro, J. L. G.; Moulijn, J. A. *Stud. Surf. Sci. Catal.* **1997**, *106*, 237–244. (c) Robinson, W. R. A. M.; van Veen, J. A. R.; de Beer, V. H. J.; van Santen, R. A. *Fuel Process. Technol.* **1999**, *61*, 103–116. (d) Yasuda, H.; Sato, T.; Yoshimura, Y. *Catal. Today* **1999**, *50*, 63–71. (e) Song, C.; Ma, X. L. *Appl. Catal., B* **2003**, *41*, 207–238. (f) Tang, T.; Yin, C.; Wang, L.; Ji, Y.; Xiao, F.-S. *J. Catal.* **2008**, *257*, 125–133. (g) Wang, A.; Qin, M.; Guan, J.; Wang, L.; Guo, H.; Li, X.; Wang, Y.; Prins, R.; Hu, Y. *Angew. Chem., Int. Ed.* **2008**, *47*, 6052–6054. (h) Zhang, J.; Wang, A.; Li, X.; Ma, X. J. *Catal.* **2011**, *279*, 269–275. (i) Bag, S.; Gaudette, A. F.; Bussell, M. E.; Kanatzidis, M. G. *Nat. Chem.* **2009**, *1*, 217–224.
- (4) (a) Sun, Y.; Prins, R. *Angew. Chem., Int. Ed.* **2008**, *47*, 8478–8481. (b) Sun, Y.; Wang, H.; Prins, R. *Catal. Today* **2010**, *150*, 213–217.
- (5) (a) Landau, M. V.; Berger, D.; Herskowitz, M. J. *Catal.* **1996**, *159*, 236–245. (b) Isoda, T.; Nagao, S.; Ma, X. L.; Korai, Y.; Mochida, I. *Energy Fuels* **1996**, *10*, 1078–1082. (c) Simon, L. J.; van Ommen, J. G.; Jentys, A.; Lercher, J. A. *J. Phys. Chem. B* **2000**, *104*, 11644–11649. (d) Simon, L. J.; van Ommen, J. G.; Jentys, A.; Lercher, J. A. *J. Catal.* **2001**, *201*, 60–69. (e) Simon, L. J.; van Ommen, J. G.; Jentys, A.; Lercher, J. A. *J. Catal.* **2001**, *203*, 434–442. (f) Shantz, D. F.; auf der Günne, J. S.; Koller, H.; Lobo, R. F. *J. Am. Chem. Soc.* **2000**, *122*, 6659–6663. (g) Nash, M. J.; Shough, A. M.; Fickel, D. W.; Doren, D. J.; Lobo, R. F. *J. Am. Chem. Soc.* **2008**, *130*, 2460–2462.
- (6) (a) Lin, S. D.; Vannice, M. A. *J. Catal.* **1993**, *143*, 539–553. (b) Lin, S. D.; Vannice, M. A. *J. Catal.* **1993**, *143*, 563–572. (c) Lin, S. D.; Vannice, M. A. *J. Catal.* **1993**, *143*, 554–562. (d) Niquille-Röthlisberger, A.; Prins, R. *Catal. Today* **2007**, *123*, 198–207.
- (7) (a) Janssen, A. H.; Koster, A. J.; de Jong, K. P. *Angew. Chem., Int. Ed.* **2001**, *40*, 1102–1104. (b) Janssen, A. H.; Koster, A. J.; de Jong, K. P. *J. Phys. Chem. B* **2002**, *106*, 11905–11909. (c) van Donk, S.; Janssen, A. H.; Bitter, J. H.; de Jong, K. P. *Catal. Rev.* **2003**, *45*, 297–319. (d) de Jong, K. P.; Zečević, J.; Friedrich, H.; de Jongh, P. E.; Bulut, M.; van Donk, S.; Kenmogne, R.; Finiels, A.; Hulea, V.; Fajula, F. *Angew. Chem., Int. Ed.* **2010**, *49*, 10074–10078. (e) Tan, Q. F.; Bao, X. J.; Song, T. C.; Fan, Y.; Shi, G.; Shen, B. J.; Liu, C. H.; Gao, X. H. *J. Catal.* **2007**, *251*, 69–79. (f) Zhao, L.; Shen, B. J.; Gao, J. S.; Xu, C. M. *J. Catal.* **2008**,

258, 228–234. (g) Qin, Z. X.; Shen, B. J.; Gao, X. H.; Lin, F.; Wang, B. J.; Xu, C. M. *J. Catal.* **2011**, *278*, 266–275.

(8) (a) Xiao, F.-S.; Wang, L.; Yin, C.; Lin, K.; Di, Y.; Li, J.; Xu, R.; Su, D.; Schlögl, R.; Yokoi, T.; Tatsumi, T. *Angew. Chem., Int. Ed.* **2006**, *45*, 3090–3093. (b) Wang, L.; Zhang, Z.; Yin, C.; Shan, Z.; Xiao, F.-S. *Microporous Mesoporous Mater.* **2010**, *131*, 58–67. (c) Choi, M.; Cho, H. S.; Srivastava, R.; Venkatesan, C.; Choi, D. H.; Ryoo, R. *Nat. Mater.* **2006**, *5*, 718–723. (d) Choi, M.; Srivastava, R.; Ryoo, R. *Chem. Commun.* **2006**, 4380–4382. (e) Srivastava, R.; Choi, M.; Ryoo, R. *Chem. Commun.* **2006**, 4489–4491. (f) Choi, M.; Lee, D. H.; Na, K.; Yu, B. W.; Ryoo, R. *Angew. Chem.* **2009**, *121*, 3727–3730. (g) Cho, K.; Cho, H. S.; de Ménéral, L. C.; Ryoo, R. *Chem. Mater.* **2009**, *21*, 5664–5673. (h) Choi, M.; Na, K.; Ryoo, R. *Chem. Commun.* **2009**, 2845–2847. (i) Wang, H.; Pinnavaia, T. J. *Angew. Chem., Int. Ed.* **2006**, *45*, 7603–7606. (j) Park, D. H.; Kim, S. S.; Wang, H.; Pinnavaia, T. J.; Papapetrou, M. C.; Lappas, A. A.; Triantafyllidis, K. S. *Angew. Chem.* **2009**, *121*, 7781–7784. (k) Li, X.; Prins, R.; van Bokhoven, J. A. *J. Catal.* **2009**, *262*, 257–265. (l) Na, K.; Jo, C.; Kim, J.; Cho, K.; Jung, J.; Seo, Y.; Messinger, R. J.; Chmelka, B. F.; Ryoo, R. *Science* **2011**, *333*, 328–332.